

Studies on CO₂ Laser Micromachining on PMMA to Fabricate Micro Channel for Microfluidic Applications

Rishi Kant, Ankur Gupta and S. Bhattacharya

Abstract Microfluidic devices are highly commonplace in the field of biomedical technology, point of care diagnostics and chemical analysis. The rapid and low cost manufacturing of these devices have always been a challenge. CO₂ laser micromachining has played an important role in micro-machining of devices at a scale similar to the microfluidic devices although it renders the machined surfaces with high surface roughness. The chapter reports an initiative to do process optimization of laser micromachining technique for producing smooth machined surfaces in the micro scale devices. The chapter discusses the impact of process parameters like raster speed, laser power, print resolution etc. and its optimization using two target functions of dimensional precision and surface roughness on micro-channels made in PMMA (Poly methyl metha acrylate) substrates. The laser machined PMMA samples are analyzed using 3D-profilometry and Field emission scanning electron microscope (FESEM) for surface quality and dimensional precision. To investigate optimum process parameters of CO₂ laser for fabricating the micro-channel on PMMA with dimensional accuracy and good surface quality, Analysis of variance (ANOVA) and regression analysis is conducted. It is found that optimum surface roughness of this process is around 7.1 μm at the optimum value of the process parameters 7.5 mm/s (50 % of maximum machine limit) raster speed, 17.9 W (51 % of maximum machine limit) laser power and 1200 DPI (100 % of maximum machine limit) printing resolution. The static contact angle of the micro-machined surface has also been observed for analyzing the amenability of these channels to flow of water like fluids for micro-fluidic applications. The chapter also covers a

R. Kant (✉) · A. Gupta
Microsystems Fabrication Laboratory, IIT, Kanpur 208016, India
e-mail: dsrishikant@gmail.com

A. Gupta
e-mail: drankur@iitk.ac.in

R. Kant · A. Gupta · S. Bhattacharya
Mechanical Engineering Department, IIT, Kanpur 208016, India
e-mail: bhatacs@iitk.ac.in

review of work done by various researchers in which they developed different methodology for successful manufacturing of microfluidic devices by employing CO₂ laser micromachining.

Keywords PMMA · CO₂ laser · Micromachining · Contact angle · Microfluidics

1 Introduction

Polymeric materials are utilized for fabricating microfluidic devices as applied to diagnostics and detection principally due to their ease in fabrication, biocompatibility, optical clarity and easy conformability to features of up to micro/nano-meter scale. Microfluidic devices made in polymeric devices find wide applications in the health care sector. The high level of interest and participation of the industry in microfluidic research and development illustrate the commercial value of these devices for important and diverse applications. Thus microfluidics is poised to become one of the most dynamic segments of the MEMS/NEMS technology.

Microfluidic devices explore the envisioned applications in confined space of several micron ranges. This micron sized space further can act as a micro-channel, micro-mixer, micro pumps, micro valves and several other active or passive devices which are commonly fabricated using expensive advanced lithography processes or other processes borrowed from the microelectronic industry. Lasers are already widely used to do laser lithography and sometimes 3-D lithography although their efficacy in micro-machining of microfluidic devices is not very widely explored. Laser and some other non-traditional machining processes are being increasingly explored for a high throughput fabrication of microfluidic devices. Among all these processes the laser machining process holds a lot of promises due to its flexibility towards parameter selection, its applicability on a wide range of materials and its rapidity of manufacture. We have successfully demonstrated the utility of CO₂ laser in micromachining of Poly Methyl Methacrylate (PMMA) devices. However, the post machined surface obtained through this process is highly non-uniform and poses a variety of restrictions on the devices regarding the flow of soft biological matter through the devices so fabricated. For example, channels used for detection and counting of mammalian cells may need a very low level of roughness to prevent lysis of the analytes. Also, high level of roughness sometimes induces local eddies and vortices very close to the rough surface leading to nonspecific adsorption of soft biological species and hinders the process of re-usability of the devices and very often gives out false positive signals in detection protocols. In addition cell adhesion, non-selective protein adsorption, particle/cell aggregation, bubble generation, optical signal detection etc. is range of problems posed by rough surfaces associated with microfluidic devices.

In earlier work Lawrence and Li (2001), Nayak et al. (2008), Heng et al. (2006), Davim et al. (2008a, b), Snakenborg et al. (2004) and a variety of other authors

have investigated the roughness of CO₂ laser machined samples of PMMA and have been able to obtain roughness in the range of few microns (Lawrence and Li 2001). While applying such methodology to fabricate the features and structures of micro-fluidic devices we were highly limited in efficacy of the devices to handle soft biological fluids by virtue of the channel roughness (Kant et al. 2013). The range of roughness that has been reported in earlier work is not enough for the specific kind of microfluidic applications as discussed and therefore we were enabled to look into the process optimization aspects so that we could achieve less than 10 microns roughness and we have been quite successful and have produced 7 microns average roughness and a high level of dimensional precision by repeated process optimization and also making a hybrid step to perform surface levelling.

In the past, to improve cutting quality (Davim et al. 2008a, b) and minimization of bulges (Li et al. 2009) during machining has been carried out by various researchers. Chung and Lin (2011) reported a microchannel fabrication strategy which reduces bulges and feature size using foil assisted CO₂ laser micromachining. Their technique is able to reduce the defects such as bulges formation, clogging, resolidification and splashing phenomena in CO₂ laser micromachining of PMMA. They could reduce channel width up to 75 μm or less using this process. Li et al. (2009) developed a technique “two times of laser cutting” to eliminate the bulges near the wall of micro channel fabricated by CO₂ micromachining. They also proposed a relationship between laser process parameter and bulge height which formed during machining. They concluded that if ratio of laser power and scanning velocity of laser beam increases bulge formation height increases. Davim et al. (2008a, b) studied the cutting quality of PMMA substrate during CO₂ micromachining. They proposed that Heat affected zone (HAZ) increases with increase in laser power and decreases with increase in cutting velocity while the surface roughness increases as laser power decreases and increases of cutting velocity. Huang et al. (2010) proposed preheating of PMMA substrate at 85 °C during machining to reduce surface roughness of the chamber sidewall. However it is also required to optimize process parameter for laser ablation on PMMA which is being presented in the current work.

1.1 Theoretical Background

The first CO₂ laser was developed at Bell Labs, United States by Patel in 1964 which produced a light beam with an infrared long wavelength band at around 9.4–10.6324 μm range. We have explored the common laser heating process assuming a circular well focussed beam on the surface and tried to infer from a commonly used one dimensional heat equation to calculate the needed beam intensity to produce a thermal ablation in PMMA surface.

The laser power density ‘ I ’ varies as it propagates inside PMMA (in ‘ Z ’ direction) and follows the Beer–Lambert law which is as

$$I = I_0 e^{-\mu z} \tag{1}$$

where I_0 is initial Power density of laser beam, μ is spectral linear absorption coefficient (cm^{-1}) and z is depth. Figure 1 shows a figure schematic of the circular lasing action on the PMMA substrate.

Yuan and Das (2007) reported a mathematical model for predicting the depth and shape of micro machined channels on PMMA substrate. The depth of channel is predicted by balancing laser irradiation energy to sum of conduction energy within PMMA and energy required to break the polymer chain (i.e. conversion into monomers). The model predicts the depth of melting temperature as $H(y)$ which is the depth of ablation of the channel at a location ‘ y ’. As the spot size is assumed to be circular the ‘ x ’ coordinate automatically gets defined once the ‘ y ’ is explicitly stated.

The mathematical model is based on following assumptions:

- (i) The laser beam intensity distribution has been assumed to be Gaussian type in three dimensional space as,

$$I(x, y, z) = \frac{P}{\pi w^2(z)} e^{-[(x^2+y^2)/w^2(z)]} \tag{2}$$

$$w^2(z) = R^2 \left[1 + (\lambda z / 2\pi R^2)^2 \right] \tag{3}$$

where P is power of laser, $w(z)$ is radius of laser beam at distance z from focal waist, λ is wavelength and R is radius of laser beam.

Assuming $\lambda z / 2\pi R^2 \ll 1$ makes Eq. (3) of constant radius laser beam

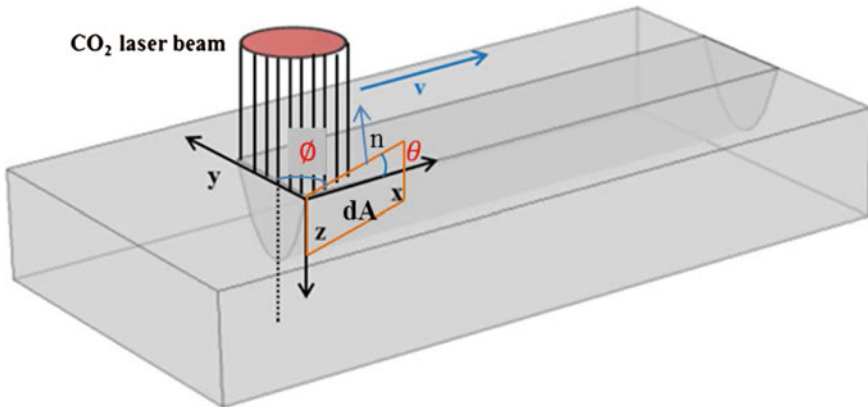


Fig. 1 CO₂ laser beam travelling with velocity v in $+x$ direction

- (ii) Energy losses due to conduction and radiation is negligible.
- (iii) Converted monomers from PMMA will affect laser beam.

Heat conduction in PMMA substrate can be expressed as

$$\frac{\partial^2 T}{\partial x^2} + \frac{\partial^2 T}{\partial y^2} + \frac{\partial^2 T}{\partial z^2} - \frac{1}{\alpha} \frac{\partial T}{\partial t} = \frac{1}{k} \tag{4}$$

where α is thermal diffusivity, k is thermal conductivity and c_p is the specific heat.

Since, $\alpha = k/c_p$ where T is the temperature at point (x, y, z) and at time t .

Due to high heat absorption coefficient of PMMA, Eq. (4) can be written by considering the direction of propagation of the laser beam (Dinger et al. 1993).

Choi and Chryssolouris (1995) proposed that three dimensional micro channel can be divided into finite surface elements which can be expressed by inclination θ in x direction and ϕ in y direction.

So the temperature distribution at surface can be achieved by solving Eq. (4) which is as

$$T(t)|_{z=0} = \frac{2I}{k} \sqrt{\frac{\alpha t}{\pi}} \tag{5}$$

If we consider energy balance for each element than input laser irradiation energy is equal to sum of energy conducted by surface elements and energy which make element into volatile products.

$$E_{laser} dx dy = E_{conduction} dA + E_{decomposition} dx dy \tag{6}$$

By geometry

$$dA = \sqrt{1 + \tan^2 \theta + \tan^2 \phi} dx dy \tag{7}$$

The laser input energy density can be expressed as

$$E_{laser} = \int_{-\infty}^{+\infty} I(x, y, z) \frac{dx}{v} \tag{8}$$

Putting the value of $I(x, y, z)$ from Eq. (2)

$$E_{laser} = \int_{-\infty}^{+\infty} \frac{P}{\pi v w^2(z)} e^{-[(x^2+y^2)/w^2(z)]} dx \tag{9}$$

On evaluation of above integral

$$E_{laser} = \frac{aP}{\sqrt{\pi R v}} * e^{-\frac{v^2}{R^2}} \tag{10}$$

The energy required to decompose PMMA into volatile MMA can be expressed as

$$E_{decomposition} dx dy = \rho L D(y) dx dy \quad (11)$$

Since laser beam is moving with v velocity in x direction, for this heat transfer can be expressed as

$$\nabla^2 T = \frac{\partial^2 T}{\partial n^2} = \frac{v}{\alpha} \frac{\partial T}{\partial x} \quad (12)$$

Since

$$\frac{\partial T}{\partial n} = \sqrt{\left[\left(\frac{\partial T}{\partial x} \right)^2 + \left(\frac{\partial T}{\partial y} \right)^2 + \left(\frac{\partial T}{\partial z} \right)^2 \right]} \quad (13)$$

Substituting above equation into

$$\frac{\partial^2 T}{\partial n^2} = \frac{v \tan \theta}{\alpha \sqrt{1 + \tan^2 \theta + \tan^2 \phi}} \frac{\partial T}{\partial n} \quad (14)$$

The energy which goes into conduction can be calculated as

$$E_{conduction} dA = \int_{-\infty}^{+\infty} \left(-k \left(\frac{\partial T}{\partial n} \right) \Big|_{n=0} \frac{dx}{v} \right) dA \quad (15)$$

Keeping the following boundary condition in Eq. (15)

$$\begin{aligned} T &= T_v \quad \text{at} \quad n = 0 \\ T &= T_0 \quad \text{at} \quad n = \infty \end{aligned} \quad (16)$$

$$\left(\frac{\partial T}{\partial n} \right) \Big|_{n=0} = \frac{v \tan \theta}{\alpha \sqrt{1 + \tan^2 \theta + \tan^2 \phi}} (T_v - T_0)$$

Now

$$E_{conduction} dA = \left[\int_{-\infty}^{+\infty} \rho c_p (T_v - T_0) \tan \theta dx \right] dx dy$$

$$E_{conduction} dA = \rho c_p (T_v - T_0) D(y) dx dy \quad (17)$$

where

P is the power of the laser beam

R is radius of laser beam

V is velocity with which laser beam travels in x direction

a is the absorptance of PMMA at the CO₂ laser wavelength of 10.6 μm

ρ is the density of PMMA

L is the latent heat of decomposition from PMMA to MMA

T_v, T_0 is decomposition and room temperature respectively.

The depth of channel is predicted by balancing laser irradiation energy to sum of conduction energy within PMMA and energy required to break the polymer chain (i.e. conversion into monomers).

Using Eqs. (6), (10), (11) and (17) and solving we get following

$$H(y) = \frac{1}{\sqrt{\pi}} \frac{aP}{Rv\rho [L + c_p (T_v - T_0)]} e^{-\frac{y^2}{R^2}} \tag{18}$$

If $H_0 = \frac{1}{\sqrt{\pi}} \frac{aP}{Rv\rho [L + c_p (T_v - T_0)]}$

Equation (18) gives a Gaussian profile for the depth of micro channel

$$H(y) = H_0 e^{-\frac{y^2}{R^2}} \tag{19}$$

Equation (19) is valid only for higher laser power at which entire underlying area of PMMA could be ablated. For low power, laser energy will not be sufficient to melt and vaporize underlying material so radius of beam (R) is not constant.

For this case depth of micro channel can be predicted as

$$H(y) = H_0 e^{-\frac{y^2}{y_{th}^2}} \tag{20}$$

where

$$y_{th} = R \sqrt{\ln \frac{2P}{\pi RvF_{th}}} \tag{21}$$

where

$$F_{th} \text{ (threshold fluence for ablation)} = I_s t_s \tag{22}$$

where I_s is given laser power density and t_s is laser irradiation time.

1.2 Mechanism of Material Removal During CO₂ Laser Micromachining of PMMA

The molecular structure of PMMA is shown in Fig. 2 which is a type of thermo-plastic. The material removal takes place by heating, melting and decomposition steps.

The decomposition of PMMA into volatile monomers (MMA) takes place at 360 °C. The decomposition reaction has been very well understood by Lippert et al. (1999) and Fig. 3 illustrates the decomposition pathway of the PMMA.

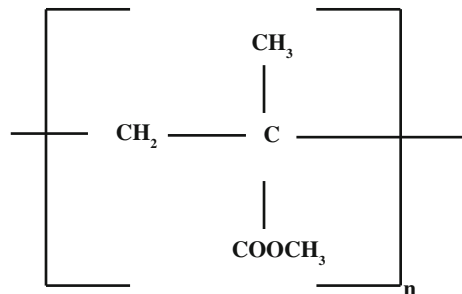
2 Experimental Set-Up

We have performed all our Laser micromachining using EPILOG WIN32 laser machine (M/S Epilog laser, USA) in laboratory conditions. All machining is done at (25 °C) room temperature condition and a positive pressure environment. The laser that we use has a maximum power of 35 W and has a total working bed size of 2 ft × 1 ft. A design of the device that needs to be laser machined is drafted using a computer assisted drawing package (Coral Draw) which is used to drive the various stepper motors with the lasing stage and also the working stage. The working stage is capable of movement in the 'z' direction and the lasing stage can operate in the raster (engraving) and vector (deep cutting) modes in the x-y plane. Figure 4 shows schematic representation of laser machining set up.

2.1 Micromachining of PMMA Substrate

PMMA is highly absorptive at the infra-red region (wavelength = 10.6 μm). Laser machining operates on the physics of photon to phonon conversion where beam matter interaction results in rapid molecular vibrations leading to generation of thermal energy. The local intensity posed by the laser is so intense (being in a very

Fig. 2 PMMA molecule's structure



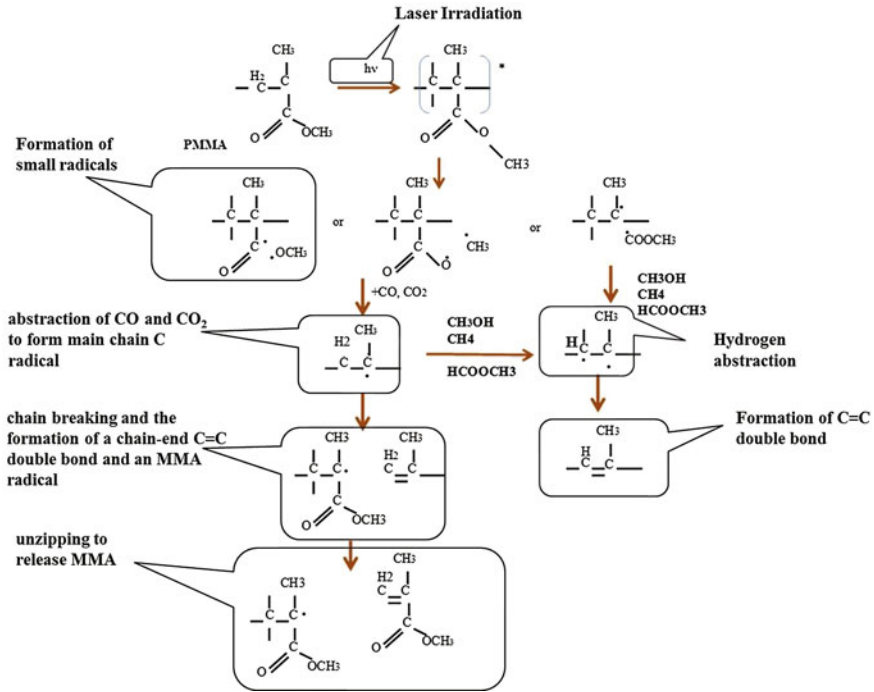


Fig. 3 Photolysis of PMMA's ester side chain

small zone) that it results in energy that is sufficient to melt and vaporize the PMMA material. The machining parameters for the laser are highly dependent on the overall feature size and correct choice of parameters leads to good dimensional accuracy. The various combinations of parameters resulting into different surface finish levels can be easily achieved using Laser processes (Nayak et al. 2008; Heng et al. 2006).

We have conducted around 30 trials with a combination of multiple parameters designed by Design Expert software. Although several trials did not scribe PMMA substrate, hence its surface roughness is not reported here and is denoted by N/A. Table 1 shows the various combinations that are proposed and the measured.

2.2 Characterization of Micro-machined PMMA Substrate

The surface roughness characterization is performed on 3D-optical profilometer (NanoMap-D, AEP Technology, USA). Various channel widths varying from 10–100 microns have been evaluated for roughness. The interferometer has optical resolution in nanometer range. The minimum area that is scanned by the system is 0.064516 mm^2 . The interferogram is used to reconstruct the topology of the surface

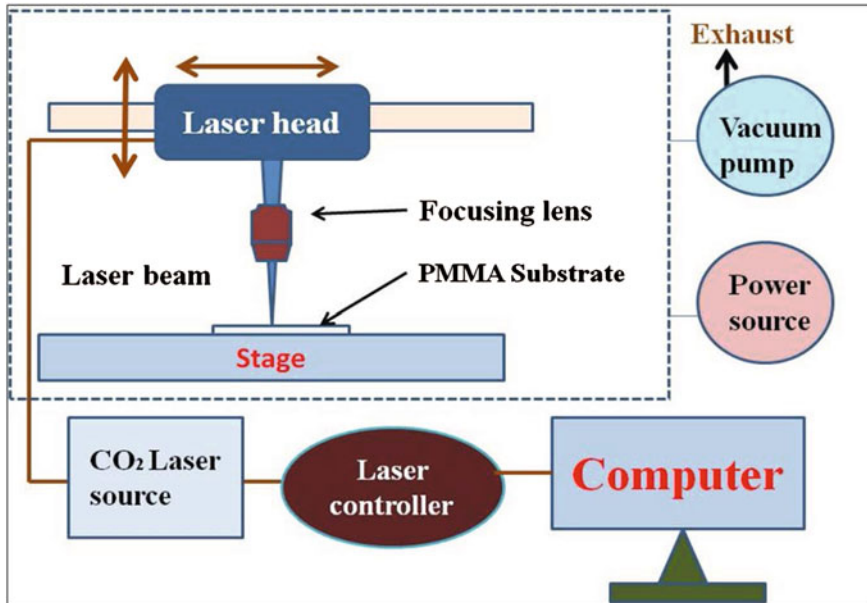


Fig. 4 Schematic diagram of CO₂ laser micromachining process

being scanned and the 3-D imaging is performed across the different micro-channel widths. The average roughness ‘Ra’ is reported to vary with the combination of different machining parameters as illustrated in Fig. 5a–j.

3 Optimization of CO₂ Laser Process Parameters for Smooth Surface

Optimization of laser machining parameters as discussed above has been performed with design of experiments (DOE) in which a central composite design (CCD) is used to fit a model. An optimum solution is extracted from the different machining parameters, including raster speed, resolution and power. Optimization was first carried out with respect to laser power and printing resolution, then with respect to speed and printing resolution and finally for speed and power. Figure 6a–c shows the output of this optimization process as contour plots. As can be seen in Fig. 6a the contour corresponding to a roughness level of 7.0647 μm starts at a base power of around 50 % and the value 7.0647 μm happens while printing at a resolution of 1200 DPI. We could not really explore a resolution more than 1200 DPI as we were limited by the machine specifications. There are of course more precise electro-mechanical stages particularly those used in scan jet printers which may be able to print at a resolution of as high as 5000 DPI and it intuitively makes sense that if the

Table 1 Details of designed parameters and measured roughness values

Resolution (DPI)	Power (%)	Speed (%)	Roughness (µm)
600	50	51	11.113
75	10	100	N/A*
1200	10	10	N/A
600	50	51	11.113
75	10	10	N/A
600	10	51	N/A
600	50	51	11.113
600	50	51	11.113
75	10	10	N/A
1200	100	10	22.003
75	100	100	N/A
600	50	51	11.113
1200	100	100	8.7607
600	50	51	11.113
600	50	100	14.461
600	50	10	N/A
75	100	10	N/A
600	50	51	11.113
75	100	100	N/A
1200	10	100	N/A
600	100	51	22.014
75	10	100	N/A
1200	10	100	N/A
75	50	51	N/A
1200	50	51	7.0647
1200	10	10	N/A
75	100	10	N/A
600	50	51	11.113
1200	100	10	N/A
1200	100	100	8.7607

Where N/A* value not available, as laser did not scribe the PMMA substrate

resolving power of the lasing head is higher than it would be able to handle higher power values while sacrificing the roughness level not too much. Similarly from Fig. 6b the minimum roughness attainable at 1200 DPI resolution limit of the system is corresponding to a speed that is 50 % of the maximum limit of the system if a similar roughness level were to be contained in Fig. 6a earlier for a combinatorial of the power as well. This gets further validated by Fig. 6c which reports a contour of 7.0647 µm average roughness corresponding to a power value of 51 % of the maximum limit of the system while maintaining the 1200 DPI level.

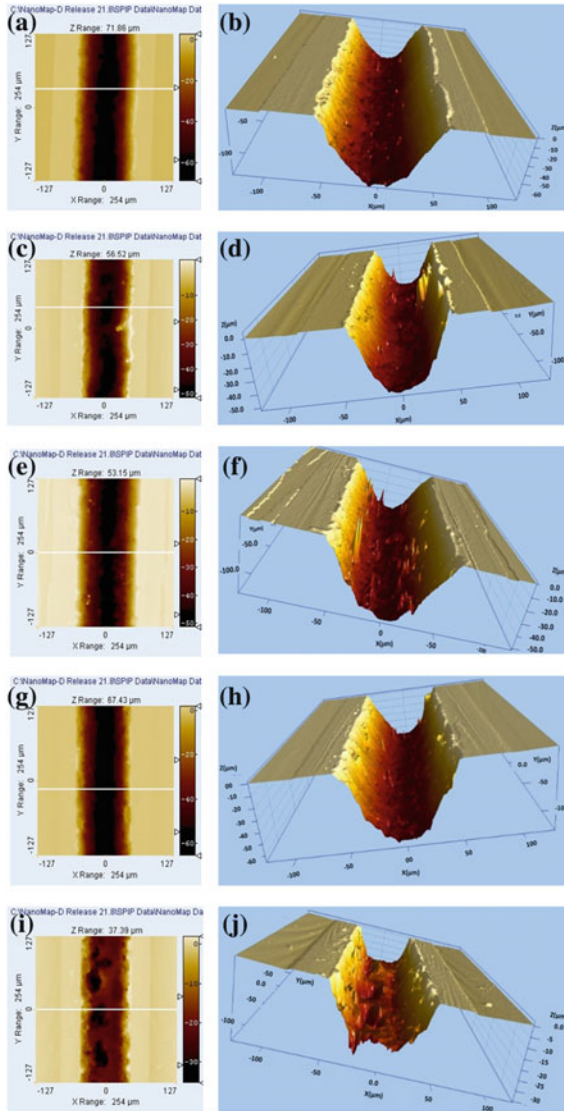
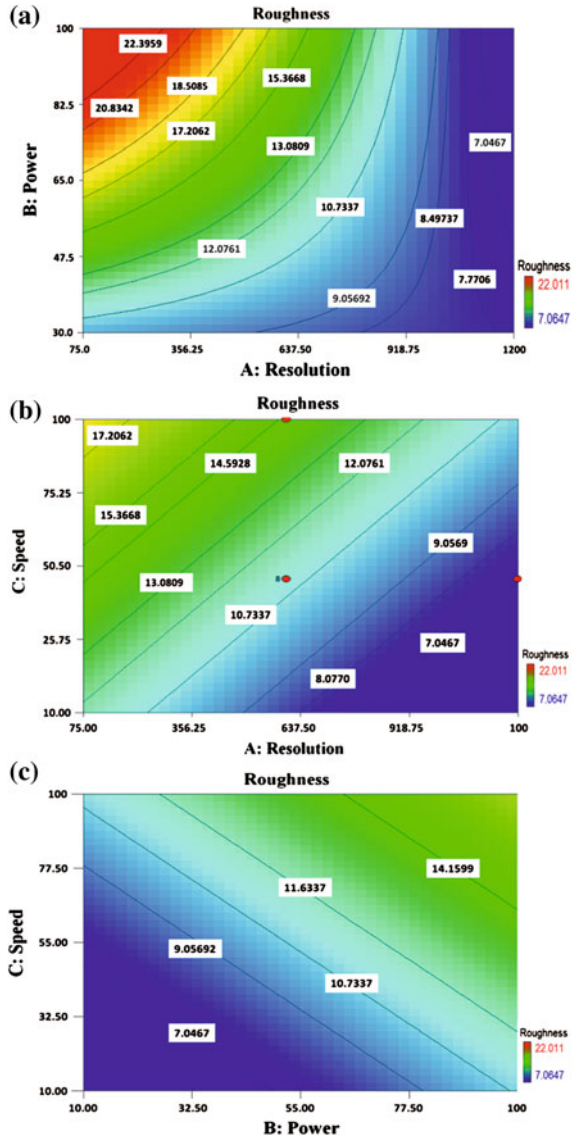


Fig. 5 **a, b** Plan view of the reconstructed image of the microchannel/3-Dimensional view (cutting parameters 1200 DPI, 17.5 W power and 7.65 mm/s rastering speed, $R_a = 7.0647 \mu\text{m}$). **c, d** Plan view of the reconstructed image of the microchannel/3-Dimensional view (cutting parameters 1200 DPI, 35 W power and 15 mm/s rastering speed, $R_a = 8.7607 \mu\text{m}$). **e, f** Plan view of the reconstructed image of the microchannel/3-Dimensional view (cutting parameters 600 DPI, 17.5 W power and 7.65 mm/s rastering speed, $R_a = 11.113 \mu\text{m}$). **g, h** Plan view of the reconstructed image of the microchannel/3-Dimensional view (cutting parameters 600 DPI, 17.5 W power and 15 mm/s rastering speed, $R_a = 22.0114 \mu\text{m}$). **i, j** Plan view of the reconstructed image of the microchannel/3-Dimensional view (cutting parameters 600 DPI, 17.5 W power and 15 mm/s rastering speed, $R_a = 14.463 \mu\text{m}$)

Fig. 6 **a** Contour plot of power and resolution for roughness. **b** Contour plot of speed and resolution for roughness. **c** Contour plot of power and speed for roughness



Therefore, we find out the optimized average surface roughness as approximately 7.06 microns and also through analysis report the speed to be 50 % of machine limit and power to be 51 % of the machine limit.

3.1 Hybrid Micro Machining to Obtain Smooth Surface

Hybrid machining strategy has been incorporated with a first step of lasing the PMMA surface followed by a wet etching of the Laser scribed PMMA micro-channel. The wet etching is carried out by using a mixture of Toluene (M/s S D Fine-Chem limited, Mumbai, India, CAS no. 108-88-3) and Methanol (M/s Loba Chemie Pvt. Ltd., Mumbai, India, CAS no. 67-56-1) in a Volume ratio of 1:4. Further samples from laser etching step are immersed totally within this solution and ultrasonicated at 42 kHz frequency (M/s Citizen Scale (I) Pvt. Ltd., Mumbai, India) inside a laminar flow hood for 15 min at room temperature. There were no significant changes in overall dimensions including depth and width of the channels/chambers while a significant reduction in the average roughness values to almost a order of magnitude. (Ra changing from 7–22 μm to 270–860 nm) as can be seen in Fig. 7.

3.2 Field Emission Scanning Electron Microscope (FESEM) Imaging of PMMA Substrate

We have also conducted field emission scanning electron microscopy (FESEM) on a laser micro-machined samples which was laser exposed using optimized machining parameter i.e. 1200 (DPI, resolution), 50 (% power) and 51 (% speed). Figure 8 shows a micrograph from the same which very clearly shows the impression left by melting and recondensation of PMMA material during machining.

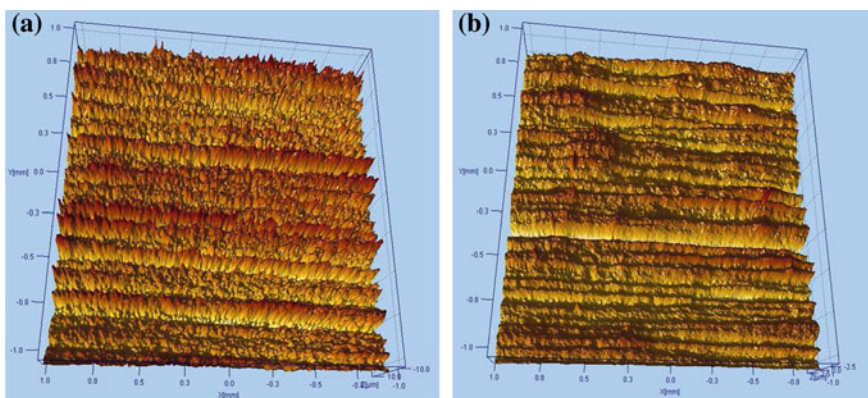
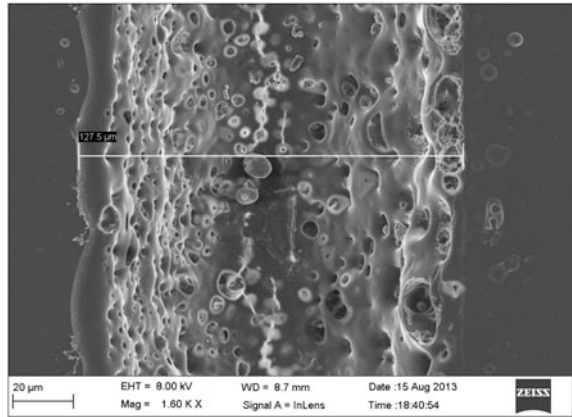


Fig. 7 **a** Reconstructed surface image of a post laser scribed PMMA surface using optical profilometer (Ra value of 7 microns). **b** Reconstructed surface image of a post wet etched PMMA surface (Ra value of 860 nm)

Fig. 8 FESEM image of micromachined PMMA substrate



4 Wettability Measurements for Microchannels

One of the main difficulties faced in working with polymeric platforms in microfluidics is the inability of the polymeric devices to drain out the fluids entrapped along embankments (Kant et al. 2013). This is more of a problem in particularly devices which actively control microscale flows like micro-pumps or valves. Therefore, it becomes highly desirable in applications involving devices whose one or more dimensions are more than 100 microns to have some kind of repulsion to water based which most of the times find useful as carrier fluids in microfluidic biodevices, Therefore the wettability characteristics become absolutely important in many situations and it is worthwhile to investigate the micro-machined channels in terms of the surface wettability. On doing such characterization we have found the surfaces whose roughness goes down to an average of 7.0647 μm owing to the lasing process and also to the Hybrid step for leveling of the surface that the static contact angle as measured on a Goniometer (M/S Dataphysics Instruments,

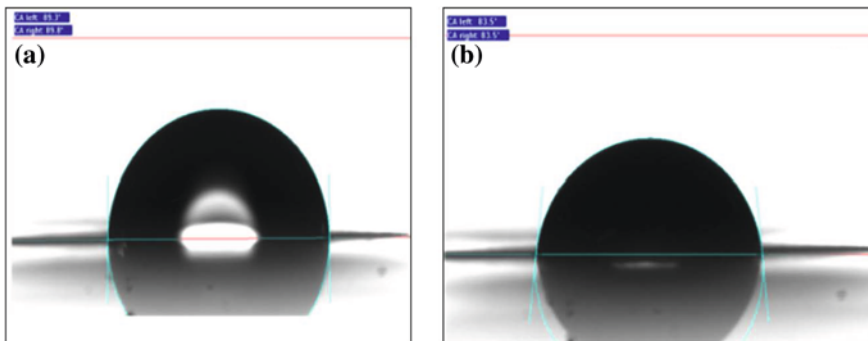


Fig. 9 a Contact angle 89.3° with water. b Contact angle 83.5° with glycerol

Germany) is quite high of the order of $83\text{--}89^\circ$ with fluids like water and glycerol (see Fig. 9). Thus the micro-machined surfaces can be considered as quite hydrophobic and therefore would find applicability in microfluidic device realization.

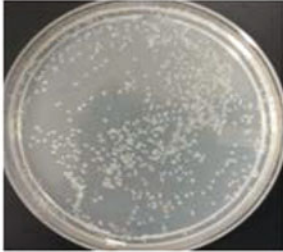

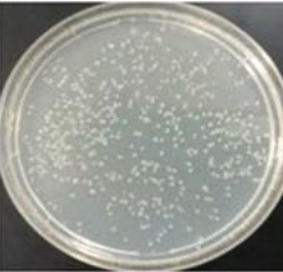
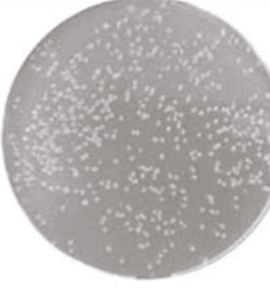
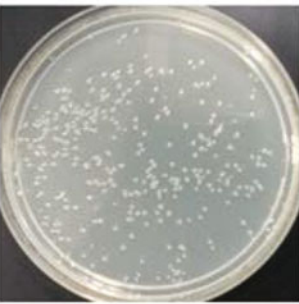
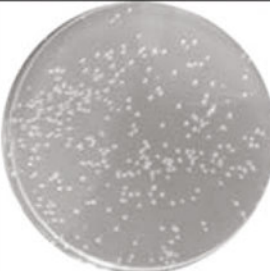
S. No.	Original image from UV Transilluminator	Processed image using Image J
1		 No of colonies 402
2		 No of colonies 398
3		 No of colonies 386

Fig. 10 The counting of cells at pre and post transport stages using image-J

4.1 Bacterial Cell Viability Studies on Surface Obtained by Hybrid Micromachining

We have also tested the PMMA surface achieved by hybrid micromachining for micro-organisms viability. We have developed piezo based micro pump for transporting bacterial cell and various experiments are conducted. The initial sample diluted to a concentration of 10^3 cfu/ml was plated using brain heart infusion (BHI) agar. The culture was diluted, plated, using transilluminator (M/s Bangalore genie) and cell counting is done using Image-J software. The initial sample recorded a count of 402 colonies and then recorded the viable colonies to be within 386–398 for three subsequent passes through the micro pumping architecture using the piezo actuator to transport the sample solution as shown in Fig. 10.

5 Conclusion

PMMA micromachining using CO₂ laser is presented and channel depth profile, reaction mechanism of material removal etc. are reviewed by thorough literature survey. We further demonstrate the basic thematic of this work by looking at the various optimization modalities which can normally be used for such a machining process in context of microfluidic device realization particularly in case of those devices which are widely used for handling devices for soft biological materials, We have optimized CO₂ laser process machining parameter (raster speed, power and resolution) to achieve smooth surface for microfluidic applications. We have further coupled this to a hybrid leveling chemical process where the overall roughness can be taken down to 7.04 μm average roughness at optimized lasing parameters with a resolution of 1200 DPI an average power of 50 % of maximum power amounting to 17.5 W and rastering speed of 51 % of machine scale amounting to 7.65 mm/s. The wettability of optimized smoothen surface is also measured using goniometer and found out to be 89° with water and 83.5° with glycerol and further analysis of viability of bacterial cells are being performed to test the claims made related to the ability of microfluidic devices to handle biological soft matter.

References

- Choi, W. C., & Chryssolouris, G. (1995). Analysis of the laser grooving and cutting processes. *Journal of Applied Physics*, 28, 873–878.
- Chung, C. K., & Lin, S. L. (2011). On the fabrication of minimizing bulges and reducing the feature dimensions of microchannels using novel CO₂ laser micromachining. *Journal of Micromechanics and Microengineering*, 21(06), 5023.

- Davim, J. P., Barricas, N., Marta, C., & Oliveira, C. (2008a). Some experimental studies on CO₂ laser cutting quality of polymeric materials. *Journal of Materials Processing Technology*, *198*, 99–104.
- Davim, J. P., Oliveira, C., Barricas, N., & Conceição, M. (2008b). Evaluation of cutting quality of PMMA using CO₂ lasers. *International Journal of Advanced Manufacturing Technology*, *35*, 875–879.
- Dinger, C., Sterkenburgh, T., Holler, T., & Franke, H. (1993). *Nonconducting Photopolymers and Applications* (pp. 278–287). San Diego, Bellingham: SPIE.
- Heng, Q., Tao, C., & Zho, T. (2006). Surface roughness analysis and improvement of micro-fluidic channel with excimer laser. *Microfluidics and Nanofluidics*, *2*, 357–360.
- Huang, Y., Liu, S., Yang, W., & Yu, C. (2010). Surface roughness analysis and improvement of PMMA-based microfluidic chip chambers by CO₂ laser cutting. *Applied Surface Science*, *256*, 1675–1678.
- Kant, R., Singh, H., Nayak, M., & Bhattacharya, S. (2013). Optimization of design and characterization of a novel micro-pumping system with peristaltic motion. *Microsystem Technologies*, *19*, 563–575.
- Lawrence, J., & Li, L. (2001). Modification of the wettability characteristics of polymethyl methacrylate (PMMA) by means of CO₂, Nd: YAG, excimer and high power diode laser radiation. *Materials Science and Engineering A*, *303*, 142–149.
- Li, J. M., Liu, C., & Zhu, L. Y. (2009). The formation and elimination of polymer bulges in CO₂ laser microfabrication. *Journal of Materials Processing Technology*, *209*, 4814–4821.
- Lippert, T., Webb, R. L., Langford, S. C., & Dickinson, J. T. (1999). Dopant induced ablation of poly(methyl methacrylate) at 308 nm. *Journal of Applied Physics*, *85*(3), 1838–1847.
- Nayak, N. C., Lam, Y. C., Yue, C. Y., & Sinha, A. T. (2008). CO₂-laser micromachining of PMMA: The effect of polymer molecular weight. *Journal of Micromechanics and Micro Engineering*, *18*(09), 5020.
- Patel, C. K. N. (1964). Continuous-wave laser action on vibrational-rotational transitions of CO₂. *Physical Review*, *136*, A1187.
- Snakenborg, D., Klank, H., & Kutter, J. P. (2004). Microstructure fabrication with a CO₂ laser system. *Journal of Micromechanics and Micro Engineering*, *14*, 182–189.
- Yuan, D., & Das, S. (2007). Experimental and theoretical analysis of direct-write laser micromachining of polymethyl methacrylate by CO₂ laser ablation. *Journal of Applied Physics*, *101*, 024901.